

REVIEW

Imaging of multifocal liver lesions in children and adolescents

Shilpa V. Hegde^a, Jonathan R. Dillman^a, Maclovio J. Lopez^b, Peter J. Strouse^a

^aSection of Pediatric Radiology, Department of Radiology, University of Michigan Health System, Ann Arbor, MI, USA;

^bDivision of Pediatric Gastroenterology, Department of Pediatrics and Communicable Diseases, University of Michigan Health System, Ann Arbor, MI, USA

Corresponding address: Jonathan R. Dillman, MD, University of Michigan Health System, Department of Radiology, Section of Pediatric Radiology, C.S. Mott Children's Hospital, 1540 East Hospital Drive, Ann Arbor, MI 48109-4252, USA.
Email: jonadill@med.umich.edu

Date accepted for publication 18 September 2012

Abstract

Multifocal liver lesions are encountered regularly in children and adolescents. By knowing the specific ultrasonographic, computed tomographic, and magnetic resonance imaging (MRI) features of benign and malignant pediatric liver lesions as well as the particular clinical setting, radiologists can frequently narrow the differential diagnosis and sometimes offer a definitive diagnosis. The purpose of this review article is to illustrate the imaging findings of numerous benign and malignant causes of multifocal liver lesions in the pediatric population.

Keywords: Liver; neoplasm; benign; malignant; children; pediatric.

Introduction

Multifocal liver lesions are encountered regularly in children and adolescents. As causes can be both benign and malignant, imaging plays an important role in attempting to noninvasively characterize such lesions, in addition to providing staging information in the setting of malignancy, predicting patient outcomes, determining which lesion (or lesions) to biopsy, and assisting with surgical planning. Although the imaging characteristics of some causes of multifocal liver lesions can overlap, necessitating percutaneous needle or surgical biopsy for a definitive diagnosis, it is sometimes possible to narrow the differential diagnosis or even arrive at an exact diagnosis based on imaging features and the specific clinical presentation, thus avoiding an invasive and costly biopsy procedure. It is important for radiologists to be able to recognize the particular imaging appearances of a wide variety of pediatric liver lesions. The purpose of this review article is to illustrate the specific imaging findings of numerous benign and malignant causes of multifocal liver lesions in children and adolescents using a multi-modality radiologic approach.

Benign multifocal liver lesions

Hepatocellular origin

Focal nodular hyperplasia

Focal nodular hyperplasia (FNH) is a hamartomatous liver lesion containing non-malignant hepatocytes, fibrous tissue, bile ducts, malformed blood vessels, and Kupffer cells^[1]. Although the exact cause of this lesion is often uncertain, it is generally thought to be due to an underlying hepatic vascular disturbance. FNHs are seen with increased frequency in long-term survivors of childhood malignancies, perhaps a complication of chemotherapy or abdominal radiotherapy^[2]. FNHs are very commonly multifocal in this setting (Figs. 1 and 2)^[2].

At ultrasonography, FNHs are circumscribed, exert a local mass effect, and may appear hypoechoic, isoechoic, or hyperechoic^[1]. On computed tomography (CT) and magnetic resonance imaging (MRI), FNHs appear as discrete lesions with circumscribed lobular margins (Figs. 1–3). On non-contrast CT, these lesions are isoattenuating/slightly hypoattenuating to normal liver, whereas they are typically mildly hypointense/isointense

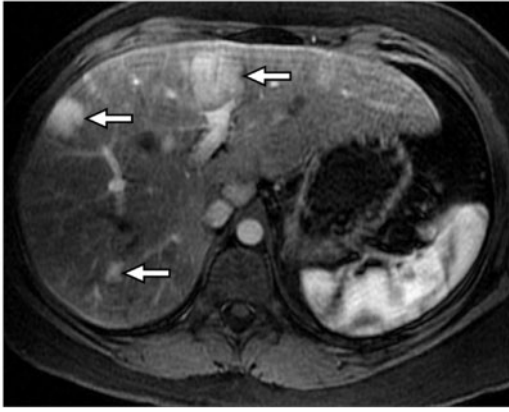


Figure 1 A 16-year-old girl with a remote history of Wilms tumor and numerous (>10) liver lesions. Axial T1-weighted three-dimensional spoiled gradient recalled fat-saturated arterial phase postcontrast MR image shows three representative hyperenhancing liver lesions (arrows) with circumscribed lobular borders. Several liver lesions were surgically biopsied with histopathology confirming the diagnosis of multiple FNHs.

and mildly hyperintense/isointense on non-contrast T1-weighted and T2-weighted MRI, respectively^[11]. FNHs generally demonstrate avid arterial phase postcontrast enhancement on both CT and MRI, and they tend to blend in with adjacent normal liver on delayed imaging (Fig. 2)^[11]. When using an MRI hepatobiliary contrast agent (e.g., Eovist; gadoxetate disodium; Bayer HealthCare, Wayne, NJ), FNHs are usually isointense or hyperintense to adjacent liver 10–20 min after contrast material injection (hepatobiliary phase) due to contrast material retention^[3,41]. However, use of such contrast material is currently an off-label practice in the pediatric population. FNHs also frequently have a central scar that is hyperintense on T2-weighted MRI and may demonstrate delayed enhancement on both CT and MRI (Figs. 2 and 3)^[11]. Early opacification of adjacent hepatic venous structures suggests lesional arteriovenous shunting of blood flow (Fig. 3).

Hepatocellular adenoma

Hepatocellular adenoma is an uncommon liver tumor during childhood that is composed of sheets of vacuo-

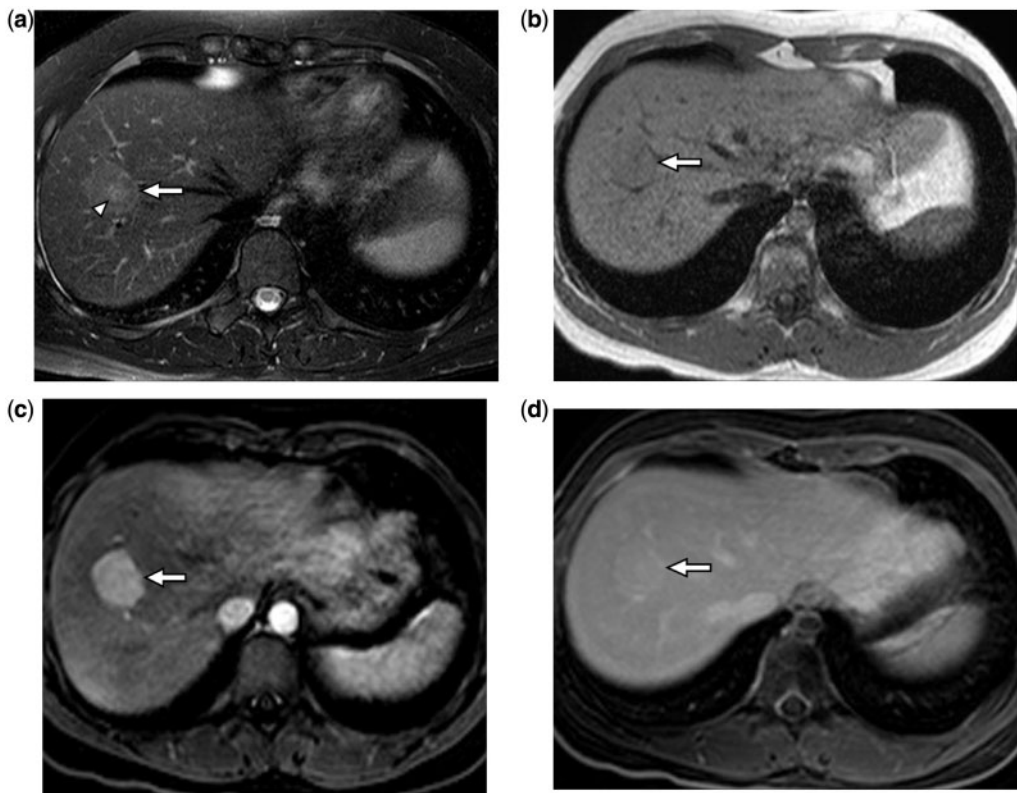


Figure 2 A 14-year-old boy with a remote history of rhabdomyosarcoma and 7 FNHs. (a,b) Axial T2-weighted fast spin echo fat-saturated and T1-weighted GRE in-phase MR images show a circumscribed lesion in the right hepatic lobe (arrows) that is subtly T2-weighted hyperintense and T1-weighted hypointense. Central stellate T2-weighted signal hyperintensity within the lesion (arrowhead) is compatible with a central scar. (c) Axial T1-weighted three-dimensional spoiled gradient recalled fat-saturated arterial phase postcontrast image demonstrates avid hyperenhancement of the lesion (arrow) compared with normal adjacent liver, whereas the lesion (arrow) appears nearly isointense to adjacent normal liver on a 5-min delayed postcontrast image (d). Other liver lesions (not shown) had similar imaging features.



Figure 3 A 13-year-old boy with incidentally detected large FNH. Late arterial phase postcontrast CT image shows a large hyperenhancing lesion within the posterior segment of the right hepatic lobe that has lobular circumscribed margins. The mass has a prominent hypoattenuating central scar that contains several small, tortuous, hepatic artery branches (arrowhead). Early opacification of the right hepatic vein (arrow) is due to arteriovenous shunting of blood. A second smaller arterially hyperenhancing lesion is not shown.

lated hepatocytes with intervening dilated sinusoids, a reduced number of Kupffer cells (compared with normal liver), and no bile ducts^[11]. Development of hepatocellular adenomas has been associated with oral contraceptive use in girls, anabolic steroid use in boys, glycogen storage disease, and congenital/acquired abnormalities of hepatic vasculature (Fig. 4)^[11]. About 20% of patients with hepatocellular adenomas have multiple lesions, particularly in the setting of predisposing conditions, such as those mentioned above^[11]. Hepatocellular adenomas may be complicated by rupture with potentially life-threatening hemoperitoneum and malignant degeneration^[5].

Recently, there have been attempts to classify hepatocellular adenomas into three distinct subtypes based on genetic, histopathologic, and radiologic features, including: (1) inflammatory hepatocellular adenomas, (2) hepatocyte nuclear factor 1 alpha (HNF-1 α)-mutated hepatocellular adenomas, and (3) β -catenin-mutated hepatocellular adenomas^[6]. The inflammatory subtype is associated with the greatest likelihood on hemorrhage; the inflammatory and β -catenin-mutated subtypes have the greatest risk of developing into hepatocellular carcinoma (up to about 10%)^[6].

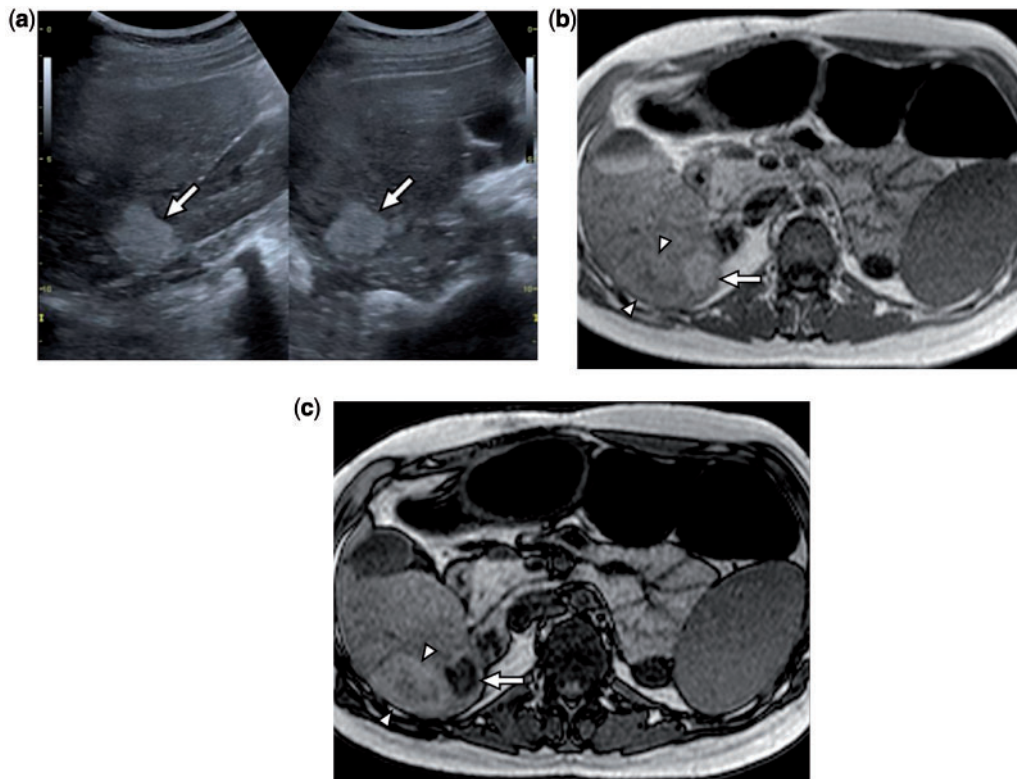


Figure 4 A 16-year-old girl with Turner syndrome, chronic portal vein occlusion, and multiple hepatocellular adenomas. (a) Composite longitudinal and transverse greyscale ultrasound images show an echogenic mass (arrows) in the posterior segment of the right hepatic lobe with circumscribed lobular margins. (b,c) Axial T1-weighted GRE in-phase and out-of-phase images demonstrate signal loss within the lesion (arrows) on out-of-phase imaging due to the presence of intracellular lipid. Percutaneous needle biopsy of several liver lesions confirmed the diagnosis of multiple hepatocellular adenomas. An additional mass (arrowheads) immediately adjacent to the presented hepatocellular adenoma was histopathologically confirmed to be a benign regenerative nodule.

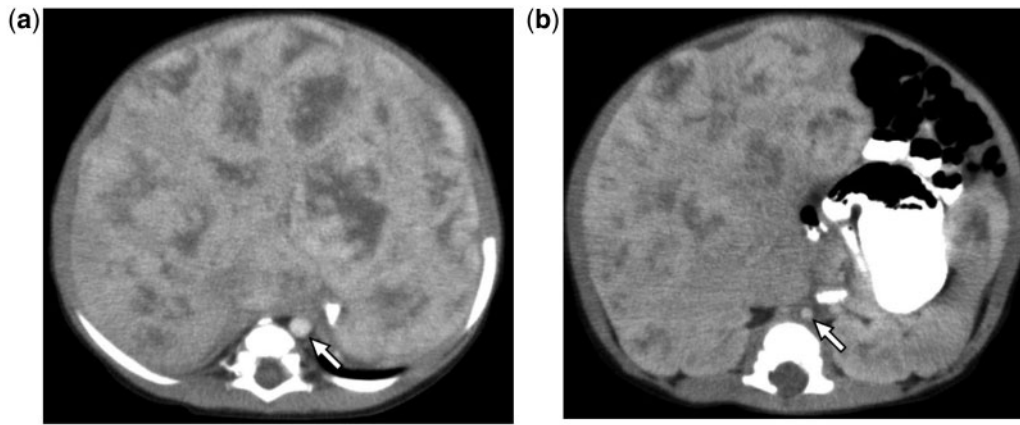


Figure 5 A 3-month-old girl with severe hepatomegaly due to numerous infantile hepatic hemangiomas. (a,b) Axial postcontrast CT images demonstrate a heterogeneous appearance of the liver due to diffuse replacement by peripherally enhancing infantile hemangiomas. The caliber of the abdominal aorta (arrows) is diminished below the level of the celiac axis, due to increased hepatic blood flow. Initial interpretation of this examination at another institution incorrectly suggested the diagnosis of hepatoblastoma.

On ultrasonography, hepatocellular adenomas can appear hyperechoic, hypoechoic, or isoechoic to adjacent liver and either homogeneous or heterogeneous (Fig. 4)^{1,51}. The appearance of these lesions depends on the echogenicity of the adjacent liver as well as how much hemorrhage, lipid/fat, and glycogen are present within the lesion. On CT, hepatocellular adenomas are commonly circumscribed and heterogeneous due to the presence of hemorrhage, lipid/fat, and rarely calcification¹¹. On MRI, many hepatic adenomas appear T1-weighted and T2-weighted hyperintense due to the presence of blood products, lipid/fat, and/or glycogen^{1,51}. Many hepatocellular adenomas commonly demonstrate arterial phase postcontrast hyperenhancement, which can persist on delayed postcontrast imaging. Washout of contrast material on delayed imaging may make these lesions indistinguishable from hepatocellular carcinoma^{16,71}. Common features that distinguish hepatocellular adenoma from FNH include: lack of central scar, T1-weighted gradient recalled echo (GRE) out-of-phase signal loss due to the presence of intracellular lipid (Fig. 4), and lack of contrast material retention on delayed imaging when using a hepatobiliary contrast agent³¹. However, inflammatory hepatocellular adenomas generally show no significant signal loss on out-of-phase compared with in-phase T1-weighted GRE images⁶¹.

Non-hepatocellular origin

Infantile hepatic hemangioma

Infantile hepatic hemangiomas are benign mesenchymal tumors composed of numerous thin-walled vascular channels and intervening fibrous stroma and that are GLUT1

immunoreactive^{1,81}. These lesions can be associated with cutaneous as well as other vascular lesions (e.g., airway)^{1,91}, and they are usually diagnosed under 6 months of age⁹¹. Infantile hepatic hemangiomas frequently enlarge rapidly and then spontaneously regress, and 50% or more of cases are multifocal based on the literature (Figs. 5 and 6)¹¹. It is possible that many solitary focal infantile hepatic hemangiomas reported in the past are actually rapidly involuting congenital hemangiomas (RICHs), a GLUT1 negative lesion. Hepatic hemangiomas (as well as other vascular lesions, such as Kaposiform hemangioendotheliomas and tufted angiomas) occurring during the infantile period have been associated with congestive heart failure from arteriovenous shunting of blood flow, bleeding tendency due to consumptive coagulopathy (Kasabach-Merritt syndrome), hypothyroidism due to increased levels of type 3 iodothyronine deiodinase, abdominal compartment syndrome, and fulminant hepatic failure^{11,10,111}.

On ultrasonography, infantile hepatic hemangiomas usually appear as one or multiple well-defined masses with circumscribed lobular margins (Fig. 6). On occasion at imaging, the liver may be diffusely involved mimicking more aggressive processes, such as hepatoblastoma (Fig. 5) or metastatic neuroblastoma. Although sonographic echogenicity can be variable, most infantile hepatic hemangiomas are hypoechoic¹¹. Echogenicity and echotexture may be either homogeneous or heterogeneous depending on the presence or absence of calcification, central necrosis, and fibrosis¹¹¹. Color Doppler evaluation typically shows relatively hypervascular lesions, and spectral Doppler interrogation may show evidence of arteriovenous shunting¹¹¹. On non-contrast MRI, these lesions are typically T1-weighted hypointense and strikingly T2-weighted hyperintense (Fig. 6)¹¹¹.

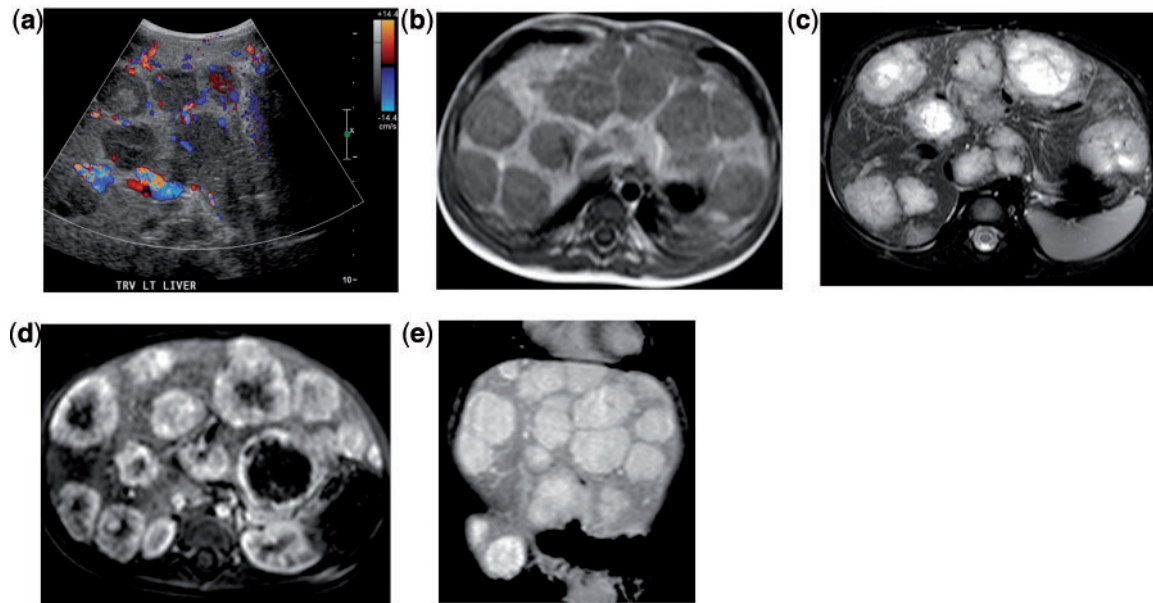


Figure 6 A 9-month-old girl with hepatomegaly and numerous infantile hepatic hemangiomas. (a) Color Doppler image through the left lobe of the liver shows multiple predominantly hypoechoic circumscribed masses with adjacent increased vascularity. (b,c) Axial T1-weighted and T2-weighted fast spin echo fat-saturated images reveal numerous circumscribed T1-weighted hypointense and T2-weighted hyperintense liver lesions. (d,e) Axial arterial phase and coronal delayed phase T1-weighted three-dimensional spoiled gradient recalled fat-saturated postcontrast MR images show early peripheral enhancement of the lesions with complete central fill-in over time.

Postcontrast MRI (or CT) typically shows either continuous or discontinuous peripheral early phase hyperenhancement, followed by progressive centripetal enhancement on delayed imaging (Fig. 6)^[1,11]. This pattern of postcontrast enhancement is particularly evident during the proliferative phase of these lesions. Flow voids within these lesions and adjacent liver as well as an abnormally small caliber of the abdominal aorta below the celiac axis may be observed due to increased hepatic blood flow (Fig. 5).

Hepatic infection

Hepatic abscesses are often multifocal and on occasion can mimic neoplasm. Multifocal hepatic abscesses can be pyogenic, fungal, or parasitic (e.g., echinococcal, amoebic)^[12]. Pyogenic abscesses in children are often the result of portal venous seeding of bacteria from an intra-abdominal infectious source (e.g., an intra-abdominal abscess due to Crohn disease or chronic perforated appendicitis), ascending cholangitis, or chronic granulomatous disease^[13,14]. Fungal hepatic abscesses are most commonly due to systemically disseminated *Candida albicans*, and are typically seen in immunosuppressed or neutropenic children, such as those with acute leukemia^[14,15]. Fungal abscesses may also affect other organs, such as the spleen^[14,16].

On ultrasonography, pyogenic abscesses can demonstrate variable echogenicity^[14]. Internal echogenic

contents may be due to septations, debris or gas. On CT, these lesions are typically centrally hypoattenuating, have circumscribed or irregular margins, and demonstrate variable peripheral enhancement^[14] (Fig. 7). Pyogenic abscesses are most commonly hypointense and hyperintense on T1-weighted and T2-weighted MR images, respectively, and they classically restrict diffusion on diffusion-weighted imaging. Variable amounts of perilesional edema may be observed on T2-weighted images^[14], and intralesional gas can be detected on both CT and MRI on occasion (Fig. 7). In the setting of chronic granulomatous disease, multifocal hepatic abscesses may have a relatively solid appearance making them difficult to distinguish from metastatic disease or hepatic lymphoma.

On ultrasonography, fungal abscesses (or microabscesses) most commonly present as multiple small (<1–2 cm) round hypoechoic liver and splenic lesions^[14]. With time and normalization of the patient's white blood cell count, a target or bull's eye appearance (echogenic center and hypoechoic rim) can develop that is usually pathognomonic for fungal infection in the appropriate clinical setting (Fig. 8)^[14]. On CT and MRI, fungal liver abscesses typically present as multiple small non-specific lesions with variable enhancement^[14]. In particular, MRI may be useful for attempting to differentiate acute, subacute treated, and chronic healed fungal disease within the liver^[16].

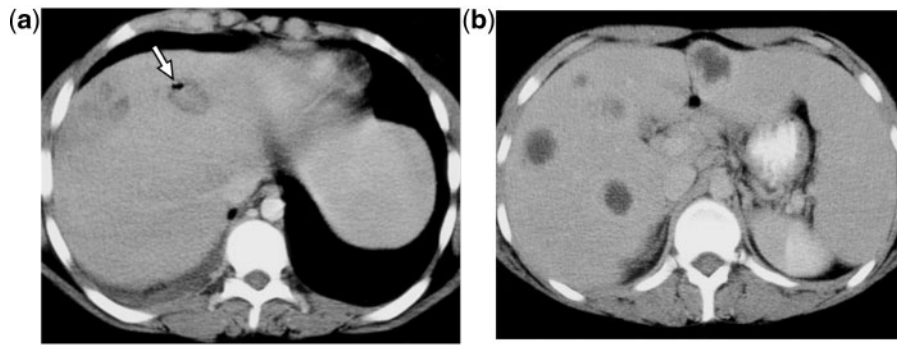


Figure 7 A 16-year-old boy with Crohn disease. (a,b) Axial postcontrast CT images through the upper abdomen demonstrate multiple low attenuation liver lesions. A single lesion contains gas (arrow). Image-guided aspiration confirmed the diagnosis of multiple hepatic pyogenic abscesses.

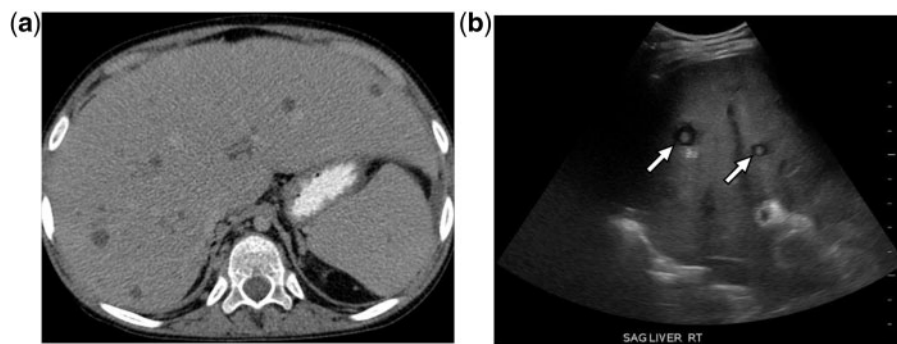


Figure 8 A 10-year-old boy with Down syndrome, acute leukemia, and systemic candidiasis. (a) Axial CT image shows multiple non-specific small round low attenuation liver lesions. (b) Longitudinal greyscale ultrasound image shows multiple target lesions (arrows) within the liver, consistent with fungal abscesses.

Malignant multifocal liver lesions

Hepatocellular origin

Hepatoblastoma

Hepatoblastoma is the most common primary liver malignancy in children, arising from primitive embryonic liver cells^[17]. Clinically, most affected children are under 5 years of age (median age is about 18 months) and present with abdominal enlargement and an abnormally increased serum alpha-fetoprotein level^[17]. Hepatoblastomas occur with increased frequency in former preterm/very-low-birth-weight children as well as those affected by Beckwith–Wiedemann syndrome and familial adenomatous polyposis syndrome (including Gardner syndrome)^[17,18]. Although about 80% present as a solitary mass, about 20% are multifocal with a variable number of satellite lesions^[17]. Multifocal hepatoblastoma is associated with reduced event-free survival, and may require total hepatectomy and subsequent liver transplantation (in the absence of contraindicative metastatic disease)^[19,20].

On imaging, hepatoblastomas present as variably sized, circumscribed, lobular lesions that have the potential to replace most of the liver and cause substantial hepatomegaly. The echogenicity and echotexture of these tumors on ultrasonography is variable, and areas of internal focally increased echogenicity with posterior acoustic shadowing suggest the presence of calcification (or bone)^[17]. On CT, hepatoblastomas are typically predominantly low attenuation, although areas of hyperenhancement may be present (especially along the periphery and septations)^[17,21]. Discrete chunky calcifications (or osseous foci) may be noted (Fig. 9)^[21]. These tumors can appear homogeneous or heterogeneous on MRI, although they are predominantly T2-weighted hyperintense and T1-weighted hypointense^[17]. Portal and hepatic venous structures should be assessed for tumor thrombus, and upper abdominal lymph nodes should also be evaluated for potential metastatic spread. Delayed phase postcontrast MRI using a hepatobiliary contrast agent has recently been shown to be beneficial for demonstrating the relationship of the tumor with the portal and hepatic veins and for identifying

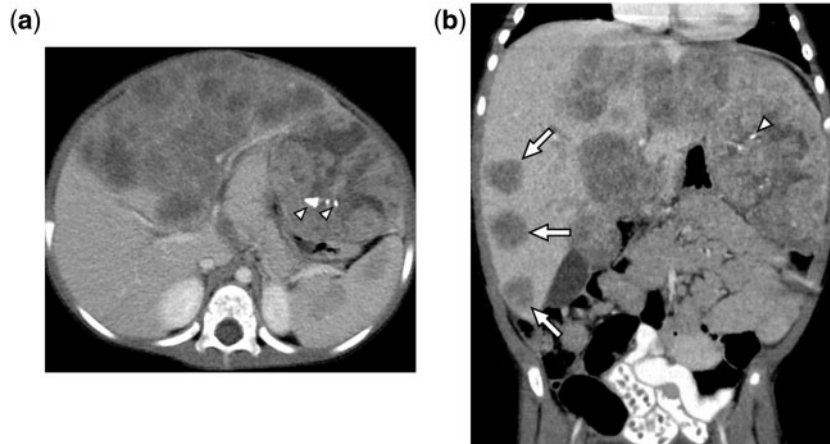


Figure 9 A 1-year-old boy with increasing abdominal distention due to multifocal hepatoblastoma. (a,b) Axial and coronal reformatted postcontrast CT images show a large, heterogeneous, predominantly low attenuation mass replacing much of the liver. The liver is also enlarged. A few satellite lesions (arrows) are present within the right hepatic lobe, and areas of focal ossification (histopathologically proven) are present within the left hepatic lobe lateral segment (arrowheads).

Table 1 PRETEXT staging system for primary malignant liver tumors in children (revised in 2005)^[23]

| PRETEXT number | Definition |
|----------------|--|
| I | One section is involved and three adjoining sections are free |
| II | One or two sections are involved, but two adjoining sections are free |
| III | Two or three sections are involved, and no two adjoining sections are free |
| IV | All four sections are involved |

intrahepatic satellite lesions, both factors that directly affect clinical management^[22].

The International Childhood Liver Tumor Strategy Group (SIOPEL) designed the PRETEXT staging system for primary malignant liver tumors in children, which was last revised in 2005^[23]. This staging system, which is primarily used in hepatoblastoma and which has good interobserver reliability, divides the liver into four sections (left lateral, left medial, right anterior, and right posterior). A PRETEXT number is designated by subtracting the highest number of contiguous sections not involved by tumor from 4 (Table 1). This system also assists with risk stratification, surgical planning, and predicts expected surgical difficulty^[23].

Hepatocellular carcinoma

Hepatocellular carcinoma (HCC) is the second most common primary liver malignancy in children after hepatoblastoma, and it is the most common in older children^[17]. In the pediatric population, these tumors, which are of hepatocyte origin, usually occur over the age of 5 years in individuals with chronic liver disease, such as viral hepatitis, progressive familial intrahepatic cholestasis, hereditary tyrosinemia, galactosemia, and

glycogen storage disease type 1^[17]. The level of serum alpha-fetoprotein is abnormally increased in about 70% of cases^[17]. Although HCCs are most often solitary, they can be multifocal or diffusely infiltrative^[17]. The fibrolamellar variant of HCC is observed in adolescents and young adult patients. Affected patients classically have no underlying liver disease, and the serum alpha-fetoprotein level is usually normal. Fibrolamellar HCC most often presents as a large solitary mass (although satellite lesions may be noted in up to 15% of cases)^[17,24–26]. Recent literature has shown that children with fibrolamellar HCC have a similar prognosis as those with conventional HCC^[24].

On ultrasonography, pediatric HCCs tend to be large, heterogeneous masses. On postcontrast CT and MRI, these lesions commonly demonstrate areas of arterial phase hyperenhancement with rapid wash out on delayed phase imaging, similar to the pattern seen in adult HCC patients^[17]. On delayed postcontrast MRI using a hepatobiliary contrast agent, HCCs (unless well-differentiated) typically appear hypointense to adjacent liver^[4]. These tumors generally appear hyperintense on non-contrast T2-weighted MRI (Fig. 10), while their non-contrast T1-weighted MRI appearance is variable and often heterogeneous due to the presence of intralésional

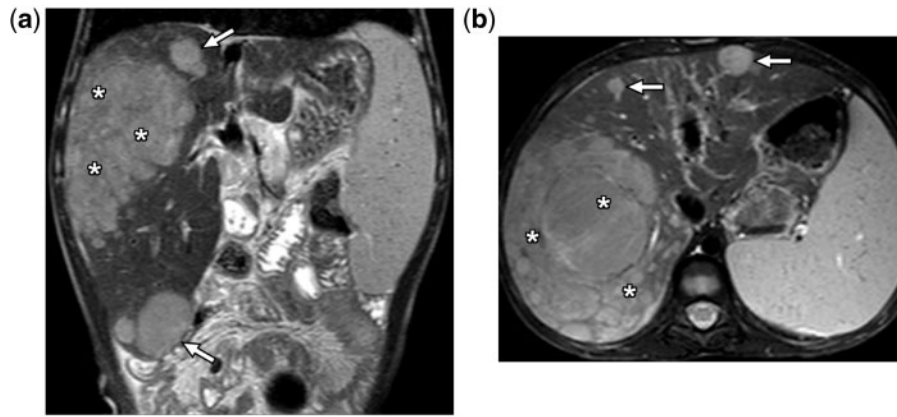


Figure 10 An 8-year-old boy with progressive familial intrahepatic cholestasis and multifocal hepatocellular carcinoma. (a,b) Coronal and axial T2-weighted MR images show a dominant mass (*) within the right hepatic lobe that is hyperintense to adjacent liver parenchyma. Scattered satellite lesions are also present (arrows). Enlargement of the spleen is due to long-standing portal hypertension secondary to the patient's underlying chronic liver disease.

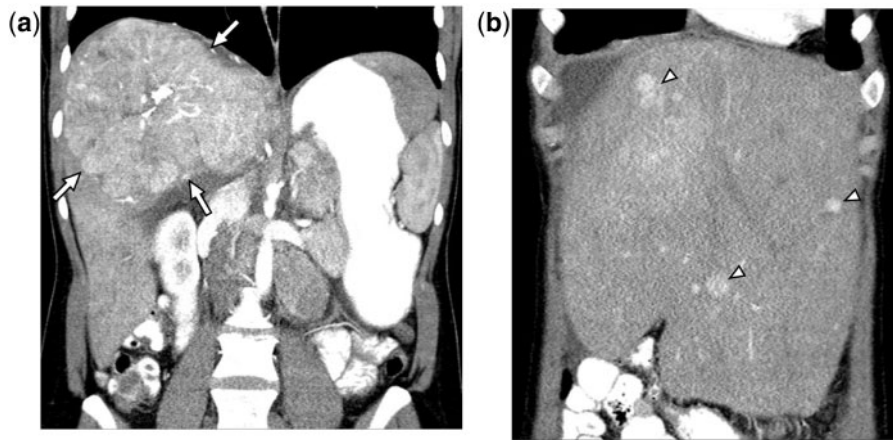


Figure 11 A 19-year-old woman with progressive abdominal distention due to fibrolamellar hepatocellular carcinoma. (a,b) Coronal reformatted postcontrast CT images show a large, circumscribed, lobular hyperenhancing mass (arrows) within the right hepatic lobe that contains central calcification. The liver is markedly enlarged, and scattered arterially hyperenhancing satellite lesions are present throughout the liver (arrowheads).

hemorrhage, necrosis, copper, calcification, and lipid/fat^[17]. Portal and hepatic venous structures should be assessed for tumor thrombus on both CT and MRI, and upper abdominal lymph nodes should also be evaluated for potential metastatic spread.

Fibrolamellar HCCs are generally large, circumscribed, lobulated masses that arterially hyperenhance on CT and MRI, and may contain central calcification and scarring (Fig. 11)^[25]. Satellite lesions are present in 10–15% of cases (Fig. 11)^[17]. The central scar associated with fibrolamellar HCC is typically hypointense on T2-weighted MRI, unlike that seen with FNH^[17,25]. These tumors are often at an advanced stage at the

time of diagnosis, and lymph node metastases are common^[26,27].

Non-hepatocellular origin

Epithelioid hemangioendothelioma

Epithelioid hemangioendothelioma is a rare usually low-to-intermediate grade malignant neoplasm of vascular origin^[17,28]. This malignancy most commonly affects women less than 40 years of age and may present during adolescence^[17]. Epithelioid hemangioendothelioma is frequently multicentric, commonly presenting with multiple liver and pulmonary lesions. Lymph node

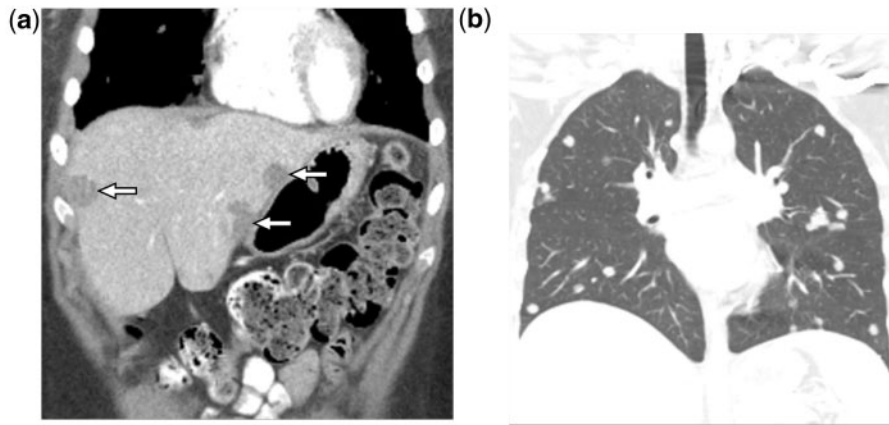


Figure 12 A 16-year-old girl with epithelioid hemangioendothelioma. (a) Coronal reformatted postcontrast CT image shows multiple non-specific hypoenhancing peripheral liver lesions (arrows). (b) Coronal reformatted CT image through the lungs shows multiple bilateral pulmonary nodules. Percutaneous needle biopsy of a peripherally located liver lesion histopathologically confirmed the diagnosis of epithelioid hemangioendothelioma.



Figure 13 A 12-year-old girl with a history of chronic immunosuppression due to inflammatory bowel disease and primary hepatic large B-cell lymphoma. Axial postcontrast CT image reveals multiple predominantly low attenuation liver lesions, some of which contain central enhancement giving rise to a target appearance. The spleen is also enlarged.

involvement is rarely seen^[17]. Unlike the much more aggressive angiosarcoma, this neoplasm usually has an indolent although somewhat unpredictable course with an overall mean life expectancy after diagnosis of more than 10 years^[29].

On imaging, epithelioid hemangioendothelioma can present with one or more liver lesions (Fig. 12)^[17,30]. Initially, lesions are usually peripherally located within the liver and may be associated with capsular retraction; lesions enlarge and coalesce with progression^[16,29]. On ultrasonography, individual lesions generally appear solid and hypoechoic^[31]. On postcontrast CT and MRI, lesions sometimes demonstrate peripheral enhancement with centripetal fill-in over time^[30]. Although biopsy may be needed to confirm the diagnosis, additional

involvement of the lungs (Fig. 12) and/or bones should suggest the possibility of this diagnosis.

Hepatic lymphoma

Although most hepatic involvement by lymphoma is secondary, primary lymphoma, usually non-Hodgkin lymphoma, arising from the liver may occur on rare occasions^[32]. Primary hepatic lymphoma occurs with increased incidence in immunosuppressed individuals (Fig. 13), including as part of the spectrum of post-transplant lymphoproliferative disease^[33].

On imaging, primary hepatic lymphomas can be solitary or multifocal, whereas secondary hepatic lymphomas most often present as multiple discrete non-specific

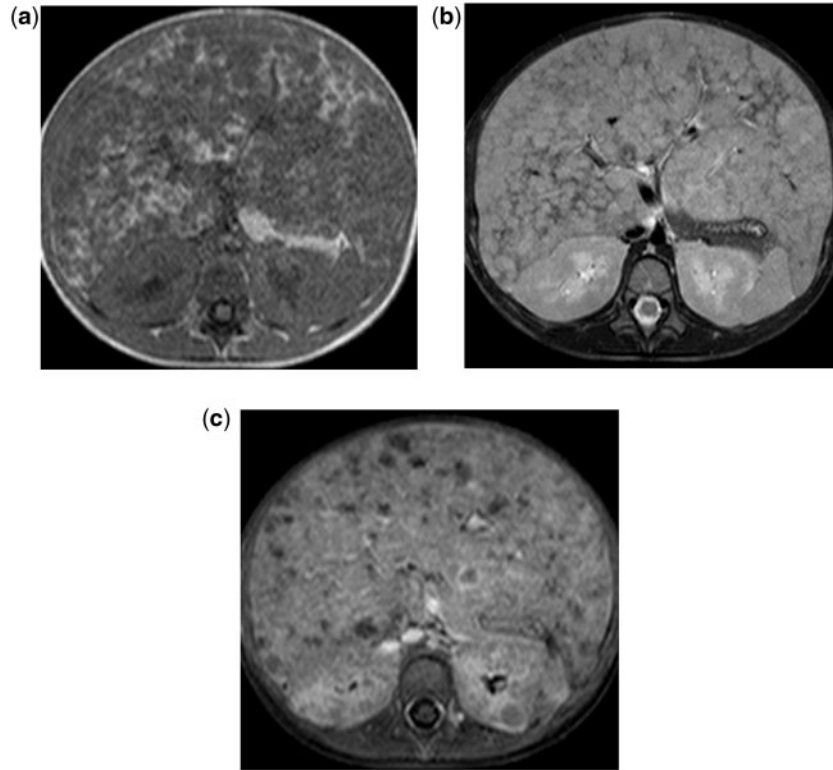


Figure 14 A 3-year-old girl with extranodal diffuse large B-cell primary lymphoma of the liver and kidneys. (a,b) Axial T1-weighted GRE in-phase and T2-weighted fast spin echo fat-saturated MR images demonstrate countless small round masses replacing almost the entire liver. The liver is diffusely enlarged. (c) Axial T1-weighted three-dimensional spoiled gradient recalled fat-saturated postcontrast MR image shows variable enhancement of the liver lesions with some appearing hypointense and others appearing isointense. A few lesions also peripherally enhance. Multiple bilateral renal lesions are also due to lymphoma.



Figure 15 A 3-month-old girl with metastatic neuroblastoma. Axial postcontrast CT image shows a left suprarenal mass (*), proven to be neuroblastoma. The liver is diffusely enlarged, and there are innumerable predominantly hypoenhancing hepatic metastases. Several hepatic metastases contain fluid-fluid levels.

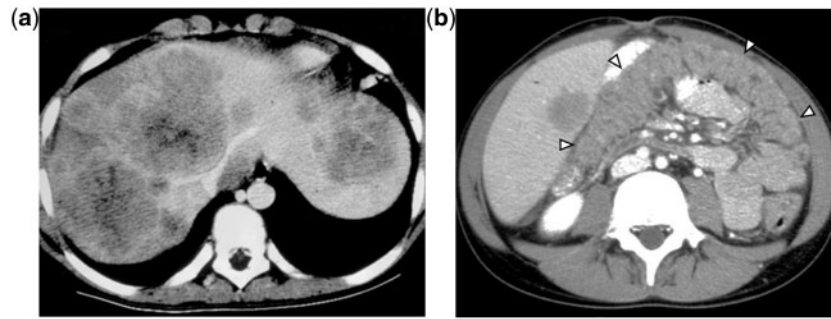


Figure 16 A 14-year-old boy with familial adenomatous polyposis and metastatic colon cancer. (a) Axial postcontrast CT image demonstrates multiple large hypoenhancing liver masses, suspicious for mucinous adenocarcinoma metastases. (b) The transverse colon (arrowheads) appears diffusely thickened due to the presence of numerous endoscopically proven colonic adenomatous polyps.



Figure 17 A 13-year-old girl with metastatic peripheral (intrahepatic) cholangiocarcinoma. Axial postcontrast CT image shows a large low attenuation mass centered in the left hepatic lobe (*). Percutaneous needle biopsy confirmed adenocarcinoma of biliary origin. Numerous additional low attenuation liver lesions are intrahepatic metastases.

lesions, sometimes mimicking metastases^[32,34,35]. On ultrasonography, hepatic lymphoma is typically hypoechoic^[34,35]. Hepatic lymphomatous deposits demonstrate variable postcontrast enhancement on CT and MRI, including occasional peripheral enhancement (Fig. 14)^[32,35].

Metastatic disease

Numerous pediatric neoplasms metastasize to the liver, typically via a hematogeneous route. Hepatic metastases are usually multiple and readily visible on ultrasonography, contrast-enhanced CT, and MRI. Based on the particular imaging features of hepatic metastases, the most likely primary neoplasm can sometimes be suggested. On postcontrast CT and MRI, hepatic metastases may be hypoenhancing (due to relative hypovascularity compared with adjacent normal liver) (Figs. 15–17) or hyperenhancing (due to relative hypervascularity compared with adjacent normal liver) (Figs. 18 and 19).

The presence of multiple liver lesions containing fluid-fluid levels and an adrenal mass can be seen in the setting of metastatic neuroblastoma (Fig. 15)^[36,37]. MRI using a hepatobiliary contrast agent may prove useful for evaluating the possibility of hepatic metastatic disease in the setting of multifocal liver lesions, as metastases typically hypoenhance on delayed imaging due to lack of contrast material retention^[4].

Summary

There are numerous causes of benign and malignant multifocal liver lesions in the pediatric population. By knowing the specific ultrasonographic, CT, and MRI features of benign and malignant pediatric liver lesions as well as the particular clinical setting, including patient age (Table 2), radiologists can frequently narrow the differential diagnosis. In some instances, radiologists can offer an exact diagnosis, thus avoiding an invasive and

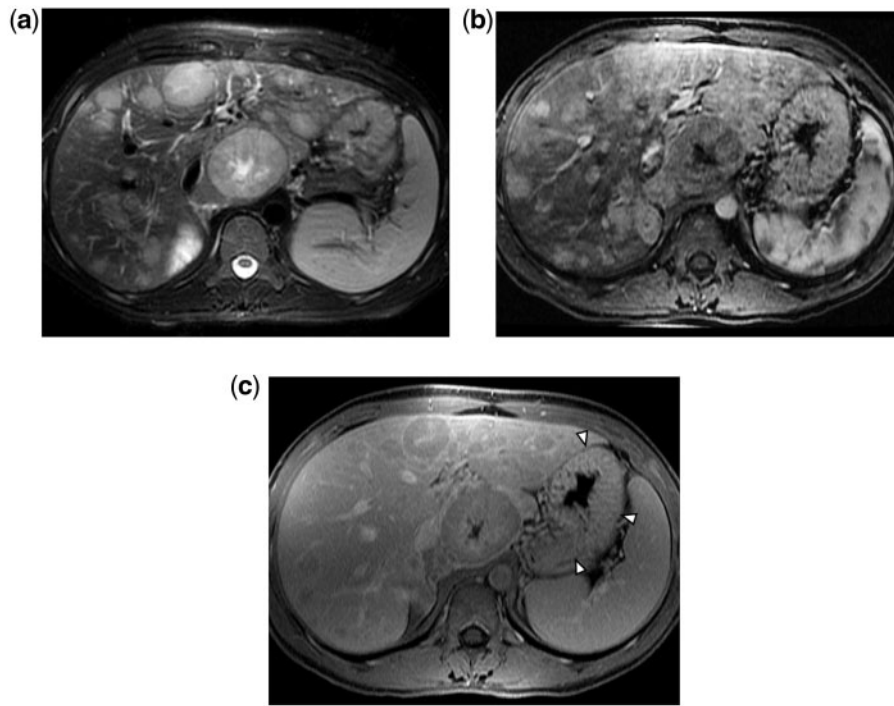


Figure 18 A 16-year-old boy with recalcitrant peptic ulcer disease due to metastatic gastrinoma (Zollinger–Ellison syndrome). (a) Axial T2-weighted fast spin echo fat-saturated MR image shows numerous hyperintense lesions throughout the liver. (b) Axial T1-weighted three-dimensional spoiled gradient recalled fat-saturated arterial phase postcontrast MR image reveals that many of the liver lesions hyperenhance, consistent with a known history of neuroendocrine tumor. (c) Axial T1-weighted three-dimensional spoiled gradient recalled fat-saturated delayed phase postcontrast MR image shows that many of the liver lesions demonstrate rapid wash out of contrast material, appearing hypointense to normal liver. Gastric fold thickening (arrowheads) is due to hypergastrinemia.

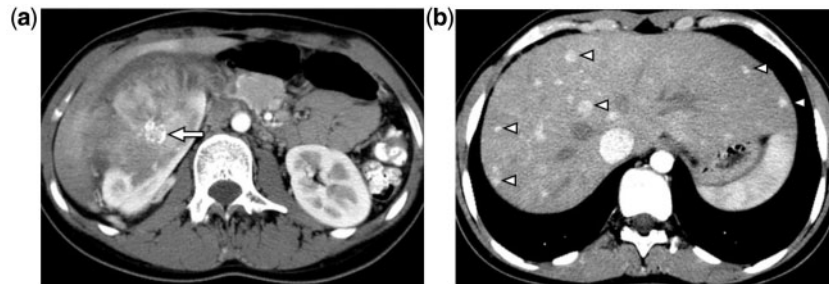


Figure 19 A 17-year-old girl with metastatic renal cell carcinoma. (a,b) Axial arterial phase postcontrast CT images show a large heterogeneous mass containing central calcification (arrow) within the right kidney as well as many small hyperenhancing metastases within the liver (arrowheads).

Table 2 Occurrence of pediatric benign and malignant multifocal liver tumors by age

| | Benign | Malignant |
|-------------|--|--|
| <2 years | Infantile hemangioma | Hepatoblastoma Metastatic disease |
| 2–5 years | Adenoma ^a | Hepatoblastoma Metastatic disease Lymphoma |
| 6–10 years | Adenoma ^a Focal nodular hyperplasia ^b | Hepatocellular carcinoma ^a Metastatic disease Lymphoma |
| 11–18 years | Adenoma Focal nodular hyperplasia ^b | Hepatocellular carcinoma Metastatic disease Lymphoma Epithelioid hemangioendothelioma Other rare neoplasms |

^aUsually associated with underlying chronic liver disease in this age group.

^bCommonly associated with a history of previous abdominal malignancy in this age group, such as Wilms tumor.

costly biopsy procedure. Imaging also continues to play very important roles in essential staging of malignancy, predicting patient outcomes, determining which lesion (or lesions) to biopsy, and operative planning.

References

- Chung EM, Cube R, Lewis RB, Conran RM. From the archives of the AFIP: pediatric liver masses: radiologic-pathologic correlation part 1. Benign tumors. *Radiographics* 2010; 30: 801–826. doi:10.1148/rg.303095173. PMID:20462995.
- Towbin AJ, Luo GG, Yin H, Mo JQ. Focal nodular hyperplasia in children, adolescents, and young adults. *Pediatr Radiol* 2011; 41: 341–349. doi:10.1007/s00247-010-1839-8. PMID:20949264.
- Grazioli L, Bondioni MP, Haradome H, et al. Hepatocellular adenoma and focal nodular hyperplasia: value of gadoxetic acid-enhanced MR imaging in differential diagnosis. *Radiology* 2012; 262: 520–529. doi:10.1148/radiol.11101742. PMID:22282184.
- Meyers AB, Towbin AJ, Serai S, Geller JI, Podberesky DJ. Characterization of pediatric liver lesions with gadoxetate disodium. *Pediatr Radiol* 2011; 41: 1183–1197. doi:10.1007/s00247-011-2148-6. PMID:21701987.
- Grazioli L, Federle MP, Brancatelli G, Ichikawa T, Olivetti L, Blachar A. Hepatic adenomas: imaging and pathologic findings. *Radiographics* 2001; 21: 877–892. PMID:11452062.
- Katabathina VS, Menias CO, Shanbhogue AK, Jagirdar J, Paspulati RM, Prasad SR. Genetics and imaging of hepatocellular adenomas: 2011 update. *Radiographics* 2011; 31: 1529–1543. doi:10.1148/rg.316115527. PMID:21997980.
- Bhayana D, Kim TK, Jang HJ, Burns PN, Wilson SR. Hypervascular liver masses on contrast-enhanced ultrasound: the importance of washout. *AJR Am J Roentgenol* 2010; 194: 977–983. doi:10.2214/AJR.09.3375. PMID:20308500.
- Mo JQ, Dimashkieh HH, Bove KE. GLUT1 endothelial reactivity distinguishes hepatic infantile hemangioma from congenital hepatic vascular malformation with associated capillary proliferation. *Hum Pathol* 2004; 35: 200–209. doi:10.1016/j.humpath.2003.09.017. PMID:14991538.
- Boon LM, Burrows PE, Paltiel HJ, et al. Hepatic vascular anomalies in infancy: a twenty-seven-year experience. *J Pediatr* 1996; 129: 346–354. PMID:8804322.
- Huang SA, Tu HM, Harney JW, et al. Severe hypothyroidism caused by type 3 iodothyronine deiodinase in infantile hemangiomas. *N Engl J Med* 2000; 343: 185–189. doi:10.1056/NEJM200007203430305. PMID:10900278.
- Kassarjian A, Zurakowski D, Dubois J, Paltiel HJ, Fishman SJ, Burrows PE. Infantile hepatic hemangiomas: clinical and imaging findings and their correlation with therapy. *AJR Am J Roentgenol* 2004; 182: 785–795. PMID:14975986.
- Kays DW. Pediatric liver cysts and abscesses. *Semin Pediatr Surg* 1992; 1: 107–114. PMID:1345476.
- Muorah M, Hinds R, Verma A, et al. Liver abscesses in children: a single center experience in the developed world. *J Pediatr Gastroenterol Nutr* 2006; 42: 201–206. PMID:16456416.
- Mortelé KJ, Segatto E, Ros PR. The infected liver: radiologic-pathologic correlation. *Radiographics* 2004; 24: 937–955. doi:10.1148/rg.244035719.
- Yen TY, Huang LM, Lee PI, Lu CY, Shao PL, Chang LY. Clinical characteristics of hepatosplenic fungal infection in pediatric patients. *J Microbiol Immunol Infect* 2011; 44: 296–302. doi:10.1016/j.jmii.2010.08.005. PMID:21524963.
- Semelka RC, Kelekis NL, Sallah S, Worawattanakul S, Asher SM. Hepatosplenic fungal disease: diagnostic accuracy and spectrum of appearances on MR imaging. *AJR Am J Roentgenol* 1997; 169: 1311–1316. PMID:9353448.
- Chung EM, Lattin GE Jr, Cube R, et al. From the archives of the AFIP: pediatric liver masses: radiologic-pathologic correlation. Part 2. Malignant tumors. *Radiographics* 2011; 31: 483–507. doi:10.1148/rg.312105201. PMID:21415193.
- Spector LG, Johnson KJ, Soler JT, Puumala SE. Perinatal risk factors for hepatoblastoma. *Br J Cancer* 2008; 98: 1570–1573. doi:10.1038/sj.bjc.6604335. PMID:18392049.
- Maibach R, Roebuck D, Brugieres L, et al. Prognostic stratification for children with hepatoblastoma: the SIOPEL experience. *Eur J Cancer* 2012; 48: 1543–1549. doi:10.1016/j.ejca.2011.12.011. PMID:22244829.
- Baertschiger RM, Ozsahin H, Rougemont AL, et al. Cure of multifocal panhepatic hepatoblastoma: is liver transplantation always necessary? *Pediatr Surg* 2010; 45: 1030–1036. doi:10.1016/j.jpedsurg.2010.01.038.
- Dachman AH, Pakter RL, Ros PR, Fishman EK, Goodman ZD, Lichtenstein JE. Hepatoblastoma: radiologic-pathologic correlation in 50 cases. *Radiology* 1987; 164: 15–19. PMID:3035605.
- Meyers AB, Towbin AJ, Geller JI, Podberesky DJ. Hepatoblastoma imaging with gadoxetate disodium-enhanced MRI—typical, atypical, pre- and post-treatment evaluation. *Pediatr Radiol* 2012; 42: 859–866. doi:10.1007/s00247-012-2366-6. PMID:22419052.
- Roebuck DJ, Aronson D, Clapuyt P, et al. 2005 PRETEXT: a revised staging system for primary malignant liver tumours of childhood developed by the SIOPEL group. *Pediatr Radiol*

- 2007; 37: 123–132. doi:10.1007/s00247-006-0361-5. PMID: 17186233.
- [24] Katzenstein HM, Krailo MD, Malogolowkin MH, et al. Fibrolamellar hepatocellular carcinoma in children and adolescents. *Cancer* 2003; 97: 2006–2012. doi:10.1002/cncr.11292. PMID:12673731.
- [25] Ichikawa T, Federle MP, Grazioli L, Madariaga J, Nalesnik M, Marsh W. Fibrolamellar hepatocellular carcinoma: imaging and pathologic findings in 31 recent cases. *Radiology* 1999; 213: 352–361. PMID:10551212.
- [26] Liu S, Chan KW, Wang B, Qiao L. Fibrolamellar hepatocellular carcinoma. *Am J Gastroenterol* 2009; 104: 2617–2624. doi:10.1038/ajg.2009.440. PMID:19638962.
- [27] Stevens WR, Johnson CD, Stephens DH, Nagorney DM. Fibrolamellar hepatocellular carcinoma: stage at presentation and results of aggressive surgical management. *AJR Am J Roentgenol* 1995; 164: 1153–1158. PMID:7717223.
- [28] Da Ines D, Petitcolin V, Joubert-Zakeyh J, Demeocq F, Garcier JM. Epithelioid hemangioendothelioma of the liver with metastatic coeliac lymph nodes in an 11-year-old boy. *Pediatr Radiol* 2010; 40: 1293–1296. doi:10.1007/s00247-009-1532-y. PMID:20112013.
- [29] Cardinal J, de Vera ME, Marsh JW, et al. Treatment of hepatic epithelioid hemangioendothelioma: a single-institution experience with 25 cases. *Arch Surg* 2009; 144: 1035–1039. doi:10.1001/archsurg.2009.121. PMID:19917940.
- [30] Chen Y, Yu RS, Qiu LL, Jiang DY, Tan YB, Fu YB. Contrast-enhanced multiple-phase imaging features in hepatic epithelioid hemangioendothelioma. *World J Gastroenterol* 2011; 17: 3544–3553. doi:10.3748/wjg.v17.i30.3544. PMID:21941423.
- [31] Miller WJ, Dodd GD 3rd, Federle MP, Baron RL. Epithelioid hemangioendothelioma of the liver: imaging findings with pathologic correlation. *AJR Am J Roentgenol* 1992; 159: 53–57. PMID:1302463.
- [32] Maher MM, McDermott SR, Fenlon HM, et al. Imaging of primary non-Hodgkin's lymphoma of the liver. *Clin Radiol* 2001; 56: 295–301. doi:10.1053/crad.2000.0649. PMID:11286581.
- [33] Honda H, Franken EA Jr, Barloon TJ, Smith JL. Hepatic lymphoma in cyclosporine-treated transplant recipients: sonographic and CT findings. *AJR Am J Roentgenol* 1989; 152: 501–503. PMID:2644774.
- [34] Gazelle GS, Lee MJ, Hahn PF, Goldberg MA, Razaat N, Mueller PR. US, CT, and MRI of primary and secondary liver lymphoma. *J Comput Assist Tomogr* 1994; 18: 412–415. doi:10.1097/00004728-199405000-00013. PMID:8188908.
- [35] Elsayes KM, Menias CO, Willatt JM, Pandya A, Wiggins M, Platt J. Primary hepatic lymphoma: imaging findings. *J Med Imaging Radiat Oncol* 2009; 53: 373–379. doi:10.1111/j.1754-9485.2009.02081.x. PMID:19695044.
- [36] Lee SY, Chuang JH, Huang CB, et al. Congenital bilateral cystic neuroblastoma with liver metastases and massive intracystic haemorrhage. *Br J Radiol* 1998; 71: 1205–1207. PMID:10434918.
- [37] Chacko J, Karl S, Sen S, Eapen A, Mathai J. Bilateral cystic adrenal neuroblastoma with cystic metastasis in the liver. *J Pediatr Surg* 2007; 42: E11–13. doi:10.1016/j.jpedsurg.2007.05.001. PMID:17706480.